Advances in Bioresearch
Adv. Biores., Vol 16 (5) September 2025: 324-337

Print ISSN 0976-4585; Online ISSN 2277-1573
Journal's URL:http://www.soeagra.com/abr.html
CODEN: ABRDC3
DOI: 10.15515/abr.0976-4585.16.5.324337

Advances in Bioresearch

ORIGINAL ARTICLE

Design, Development and Characterization of Nanoparticles Containing Atenolol

Praveen Javali R*[1], Aman Suresh T[2], Shankar Yelmame[3], Shweta Lalit Dhande[4], Dhanalakshmi P[5], Darshan HB[6], Adinarayana Andy[7], AMT Gurubasavaraj[8], Sreya Kosanam[9], Nithin Sujay KJ[10]
[1,] Department of Pharmaceutics, Faculty of Pharmacy, Sri Raghavendra College of Pharmacy, Chitradurga, Karnataka, India.
[2] Department of Pharmacy Practice, Faculty of Pharmacy, Dr. M.G.R. Educational and Research Institute, Velappanchavadi, Chennai 600077, Tamil Nadu, India.
[3] Department of Quality Assurance, Sandip Institute of Pharmaceutical sciences, Nashik, Maharashtra
[4] Department of Pharmaceutics, Sandip Institute of Pharmaceutical sciences, Nashik, Maharashtra
[5]Department of Pharmacy, Faculty of Pharmacy, Dr. M.G.R. Educational and Research Institute, Velappanchavadi, Chennai 600077, Tamil Nadu, India.
[6]Norwich Medical School, University of East Anglia, Norwich, England, United Kingdom.
[7]Pharmacy Manger, Weatherwax Family Pharmacies Inc, Spring Arbor, Michigan USA-49283
[8]Assistant Professor Department of Pharmaceutics, YSS college of Pharmacy Kudligi, Karnataka.
[9]Department of Pharmacy, Faculty of Pharmacy, Dr. M.G.R. Educational and Research Institute, Velappanchavadi, Chennai 600077, Tamil Nadu, India.
[10]Assistant Professor Department of Pharmaceutics, St.Mary's College of Pharmacy, Chitradurga.
Corresponding Author: Praveen Javali R

ABSTRACT
The present study details the design, development, and characterization of nanoparticles containing Atenolol, using synthetic polymers Eudragit RS 100 and Eudragit RSPO through the nanoprecipitation method, coupled with high-speed homogenization. The aim is to treat hypertension by enhancing the drug's oral bioavailability. The nanoparticles produced were evaluated for surface morphology, drug entrapment efficiency, differential scanning calorimetry, particle size, and Fourier transform infrared spectroscopy for in vitro drug release studies. The nanoparticles exhibited smooth, spherical surfaces, with particle sizes ranging from 612.9 nm to 923.1 nm. Drug entrapment efficiency ranged from 83.02% to 91.21%, increasing with higher polymer concentration. The in vitro drug release followed zero-order kinetics, showing maximum release over 24 hours. The FTIR spectra indicated that there were no significant deviations in the peaks when comparing the original Atenolol drug with the nanoparticles' formulation. The optimized formulation showed stability during drug entrapment efficiency, in vitro release studies, and short-term stability testing, with no significant changes observed.
Keywords: *Atenolol, Nanoprecipitation, High Speed Homogenization, Eudragit RS 100 and Eudragit RSPO*

Received 24.06.2025 Revised 09.07.2025 Accepted 21.09.2025

How to cite this article:
Praveen Javali R, Aman Suresh T, Shankar Y, Shweta Lalit D, Dhanalakshmi P, Darshan HB, Adinarayana A, AMT Gurubasavaraj, Sreya K, Nithin Sujay KJ. Design, Development and Characterization of Nanoparticles Containing Atenolol. Adv. Biores. Vol 16 [5] September 2025. 324-337

INTRODUCTION

Nanoparticles are colloidal particles characterized by sizes ranging from 10 to 1000 nm[30]. Nanoparticles possess unique physical, chemical, and biological properties compared to larger particles. Over time, nanotechnology has attracted significant attention, with nanoparticles being a fundamental aspect of this field. These particles vary in dimensions, shapes, and sizes, as well as in their material composition. They come in various shapes, sizes, and structures. Nanoparticles can have a variety of shapes, including cylindrical, spherical, tubular, conical, hollow core, spiral, flat, or irregular, with sizes ranging from 1

nanometre to 100 nanometres. The surface may be uniform or exhibit variations. They can be crystalline or amorphous, consisting of single or multiple crystals that may exist independently or in clusters(1).
Hypertension is characterized by an increase in blood pressure of unknown origin, raising the risk for cerebral, cardiac, and renal complications. More than 90% of individuals in industrialized countries are at risk of developing hypertension (blood pressure >140/90 mm Hg) during their lifetime. Hypotension is frequently linked with other cardiovascular risk factors, such as aging, obesity, diabetes, and hyperlipidemia(2).
Antihypertensive medications are primarily used to reduce the morbidity and mortality linked to hypertension and its complications. Many individuals need more than one medication to manage their hypertension effectively. Different types of antihypertensive drugs, such as diuretics, renin-angiotensin system inhibitors, calcium channel blockers (CCBs), and beta-blockers (BBs), have been proven to decrease hypertension-related complications and can be employed in initial drug therapy [33]Atenolol, a frequently used antihypertensive medication, belongs to the beta-blocker group and is categorized under BCS class III due to its high solubility and low permeability(3). Atenolol is extensively used in treating various cardiovascular conditions, including hypertension. The prevalence of hypertension has significantly increased in recent years, leading to a greater reliance on these β-blockers. Additionally, Atenolol is used to manage myocardial infarction (heart attacks), arrhythmias (rhythm disorders), and angina pectoris (chest pain)(4).

METERIAL AND METHODS

Atenolol was provided as a gift sample by Karnataka Antibiotics & Pharmaceuticals Ltd., Bangalore. Eudragit RS100 and Eudragit RSPO were acquired from SD Fine Chemicals Ltd., Mumbai, while polyvinyl alcohol was sourced from Fisher Scientifics Pvt. Ltd. Acetone was used consistently throughout the study.

METHOD:

Formulation Batches:

Accurately weigh 0.5% PVA and transfer it into a beaker, then dissolve it in 100 ml of distilled water using a magnetic stirrer until fully dissolved. Dissolve the polymers (Eudragit RS-100 and Eudragit RSPO) in an organic solvent (acetone). Dissolve 100 mg of Atenolol in distilled water. Mix the drug-polymer solution with the PVA aqueous solution using a controlled-rate syringe pump while continuously homogenizing for 1 to 1.5 hours at 5000 rpm. After homogenization, centrifuge the solution at 10,000 rpm for 20 minutes to obtain the nanoparticles. Dry the nanoparticles at room temperature for 12 hours and then collect the dried nanoparticles(5,6).

Table No. 1: Formulation table of Atenolol Nanoparticles

Formulation	Atenolol (mg)	Eudragit RS100 (mg)	Eudragit RSPO (mg)	Acetone (ml)	Polyvinyl alcohol (%)
ATL 1	100	100	-	30	0.5
ATL 2	100	150	-	30	0.5
ATL 3	100	200	-	30	0.5
ATL 4	100	250	-	30	0.5
ATL 5	100	-	100	30	0.5
ATL 6	100	-	150	30	0.5
ATL 7	100	-	200	30	0.5
ATL 8	100	-	250	30	0.5
ATL 9	100	150	150	30	0.5

Characterization of Nanoparticles:

Drug - Excipient Compatibility Study:

The compatibility study of drug and excipient were evaluated by FT-IR study(7).

FTIR Study:

The compatibility between the drug and the polymers (Eudragit RSPO and Eudragit RS100) was analyzed using an FTIR spectrophotometer (BRUKER ALPHA E). The FTIR spectra of the combined polymers and the drug Atenolol were compared with the standard FTIR spectra of the pure drug. The samples were placed in a sample holder and scanned in the spectral range from 4000 cm^{-1} to 650 cm^{-1}(8).

Surface morphology:

Surface morphology is typically examined using scanning electron microscopy. In this study, surface morphology was analyzed with a JEOL JSM-IT500 scanning electron microscope (SEM)(9).

Particle size:
Particle size and distribution were measured using a Malvern Zetasizer with the wet technique. The average particle sizes for each individual batch of nanoparticles were reported(7,10,11).
Zeta potential:
The Zeta potential is a key parameter for characterizing the surface charge properties of nanoparticles. It is measured using a Malvern Zeta analyzer(12–14).
Differential Scanning Calorimetry (DSC):
DSC thermograms of pure drugs and their Eudragit RS100 and Eudragit RSPO-loaded nanoparticles were recorded using a DSC (Shimadzu, Japan). Indium was employed as a standard to calibrate the differential scanning calorimetry for temperature and enthalpy measurements(9,15).
Drug entrapment efficiency:
The nanoparticles were isolated from the aqueous medium by ultracentrifugation at 10,000 RPM for 10 minutes. The resulting supernatant was decanted and the nanoparticles were dispersed into phosphate buffer at pH 6.8. This procedure was repeated twice to ensure the complete removal of un-entrapped drug molecules. The amount of drug entrapped in the nanoparticles was calculated by subtracting the quantity of drug in the aqueous medium from the total amount used to prepare the nanoparticles(16).

$$\text{Drug Entrapment efficiency} = \frac{\text{Amount of drug released from the lysed nanoparticals}}{\text{Amount of drug initially taken to prepare the nanoparticle}} X100$$

In Vitro release studies of Nanoparticles:
In-vitro drug release studies were performed using a USP Type II dissolution apparatus with a rotating speed of 50 revolutions per minute. The nanoparticles were placed in 900 millilitres of pH 6.8 phosphate buffer solution within the vessel, and the temperature was maintained at 37±5°C. At designated time intervals, 5 ml of the solution was withdrawn, and the same volume of fresh dissolution medium was added to the flask to maintain a constant volume (sink conditions). The withdrawn samples were analysed using a UV Spectrophotometer (SHIMADZU 1700)(17).
Kinetic modelling:
The results from the in vitro release studies of the optimized batch were analysed using various models to determine the drug release mechanism. The kinetic models applied included zero-order, first-order, Higuchi, and Peppa's equations(17).
Stability studies:
Stability testing is conducted to confirm that drug products remain suitable for use throughout their shelf life. This testing assesses how a drug's quality is affected by environmental factors such as temperature and humidity over time. The prepared nanoparticles were stored in screw-capped HDPE bottles at 40±2°C and 75% relative humidity (RH) for 45 days. After this storage period, the products were evaluated for drug entrapment efficiency and drug release, following ICH guidelines(18).

RESULTS AND DISCUSSION

Determination of λ_{max} of Atenolol
A spectrophotometric method based on the measurement of absorbance at 226.6 nm in Phosphate buffer pH 6.8 was used in the present study for the estimation of Atenolol. The method obeyed Beer's law in the concentration range of 2 - 10 µg/ml. The spectrum was recorded using a UV spectrophotometer (UV1700, Shimadzu, Japan). The results shown that table no-2, and Figure no-1.

Table No. 2: Calibration curve of Atenolol in Phosphate buffer pH 6.8

Sl. No	Concentration (µg/ml)	Absorbance (at 226.6nm) n=5	
		$\bar{x}$	RSD (%)
1.	0	0	0
2.	2	0.095	0.095 ± 0.014
3.	4	0.203	0.203 ± 0.024
4.	6	0.312	0.312 ± 0.010
5.	8	0.410	0.410 ± 0.023
6.	10	0.502	0.502 ± 0.022

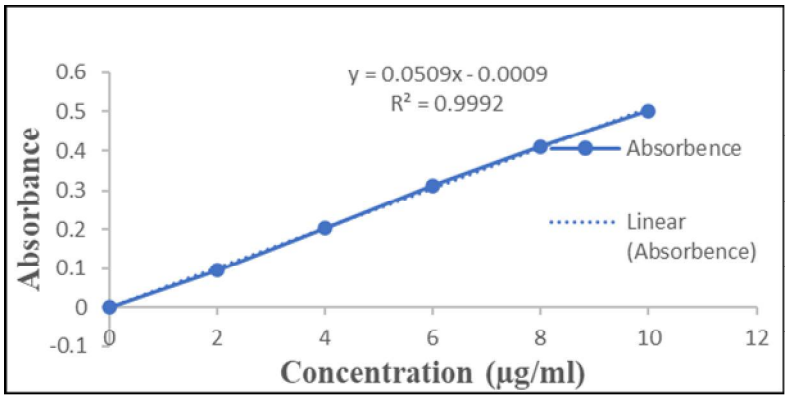

Fig No. 1: Calibration curve of Atenolol in Phosphate buffer pH 6.8

Drug - Excipient Compatibility Study

The drug polymer compatibility was studied by FTIR Spectroscopy (BRUKER ALPHA E). FTIR spectrum for pure drug and physical mixture of drug-polymers were obtained and characterized. The intense peak at 3349 cm-1 is shown due to O-H stretching. 2963 cm-1 is shown due to C-H stretching. 1633 cm-1 is shown due to C=O stretching. 1511 cm-1 is shown due to C=C stretching. 1233 cm-1 is shown due to C-O-C stretching. FTIR spectra of pure Atenolol drug and physical mixture showed corresponding peaks which indicating no interaction between polymers and drug Atenolol The results are as shown in Figure No- 2, 3, 4, and 5, and Table No- 3, 4.

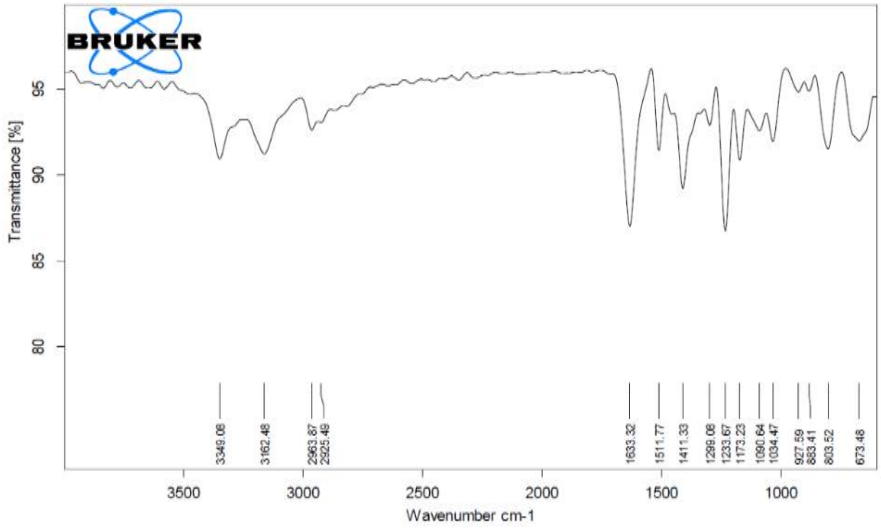

Fig No. 2: FTIR of Pure Drug Atenolol

Results of FTIR spectra's of pure drug Atenolol

Table No. 3: FTIR Spectra of Atenolol Nanoparticles shows following peaks

Peaks	Groups
3349.08	(O-H stretching)
2963.87	(C-H stretching)
1633.32	(C=O stretching)
1511.77	(C=C stretching)
1233.67	(C-O-C stretching)

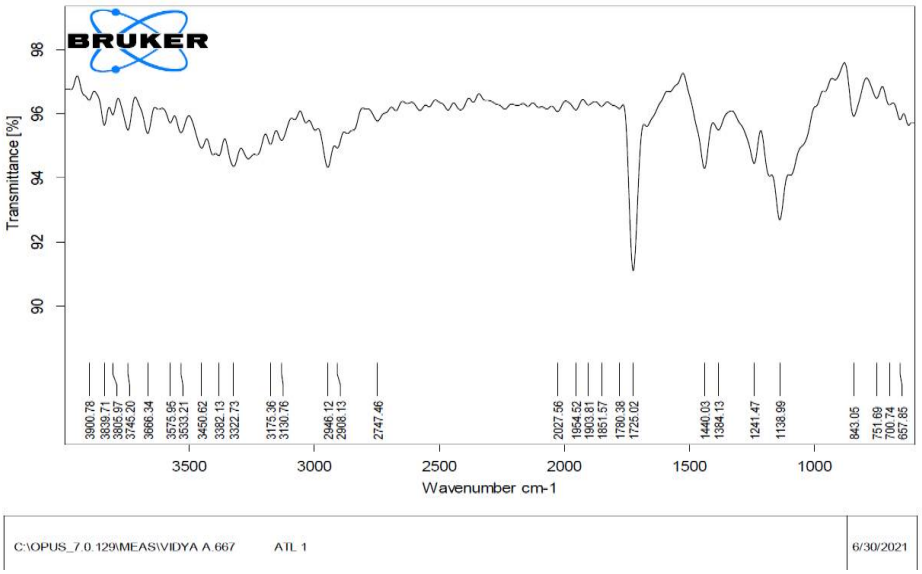

Fig No. 3: FTIR spectra of ATL 2

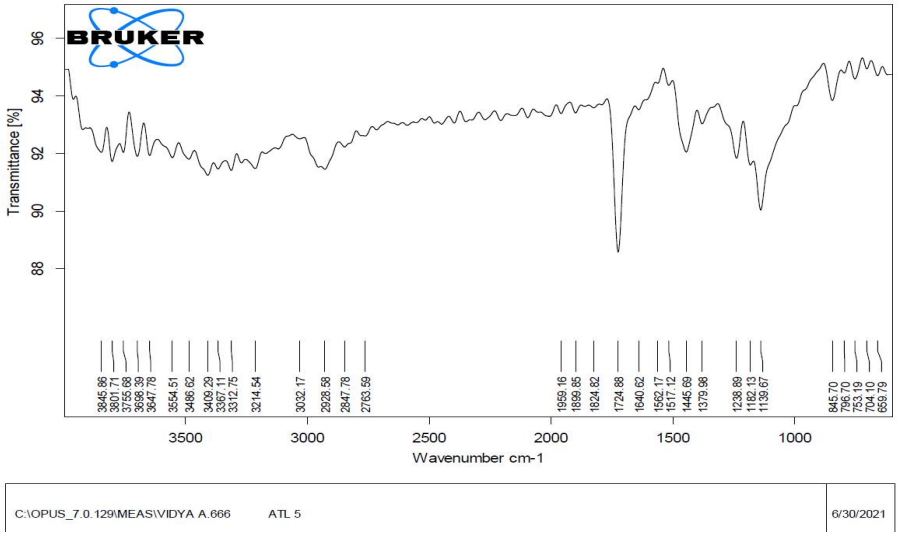

Fig No. 4: FTIR spectra of ATL 6

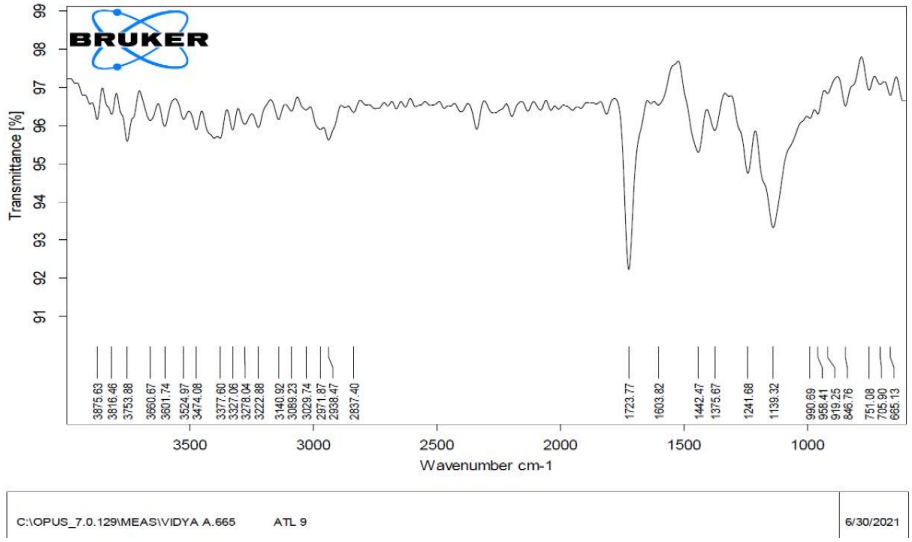

Fig No. 5: FTIR spectra of ATL 9

Results of FTIR spectra's ATL 9 formulation

Table No.4: FTIR Spectra of Atenolol Nanoparticles shows following peaks

Peaks	Groups
3327.06	(O-H stretching)
2938.47	(C-H stretching)
1723.77	(C=O stretching)
1603.82	(C=C stretching)
1241.82	(C-O-C stretching)

Scanning electron microscopy (SEM):
The surface morphology and shape of the nanoparticles were determined using a JEOL JSM-IT500 Scanning Electron Microscope. The Prepared nanoparticle formulations exhibited a spherical shape and a smooth surface, as shown in Figure No- 6, 7, and 8.

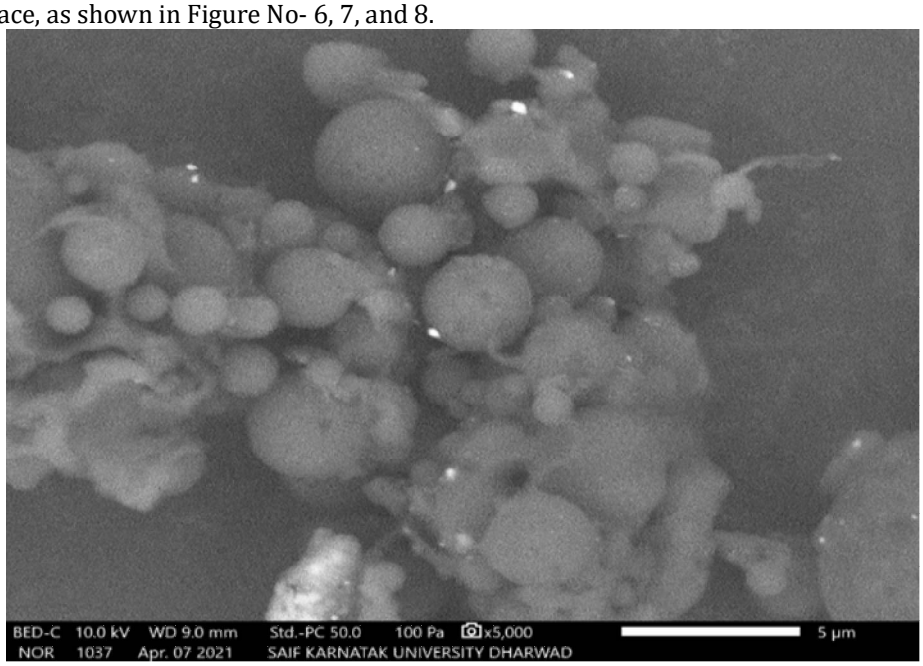

Fig No. 6: SEM images of ATL 2

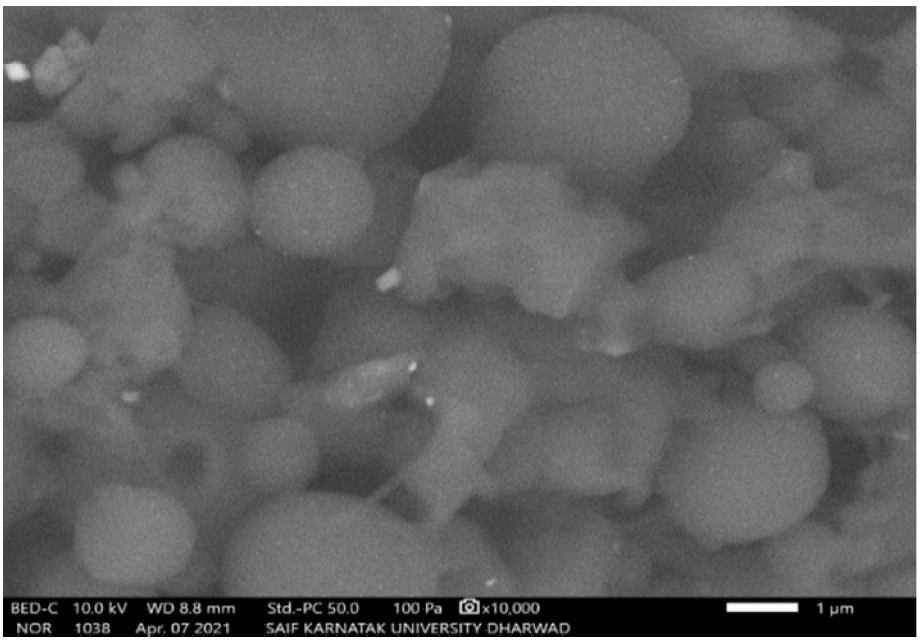

Fig No. 7: SEM images of ATL 6

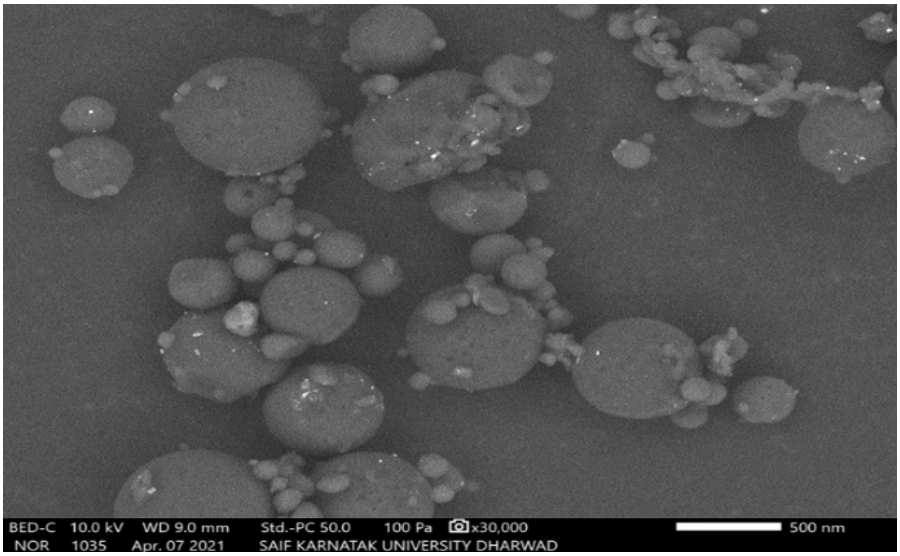

Fig No. 8: SEM images of ATL 9

Particle size analysis:

The particle size of the Prepared Atenolol nanoparticles was analyzed using a particle size analyzer (Malvern Zetasizer), and the size of the prepared nanoparticles were found in the ranged from 612.9 to 923.1 nm. and the drug entrapment efficiency (EE) of the Prepared Atenolol Nanoparticles were found in the range of 83.30% to 91.21%. Here the drug entrapment efficiency of prepared Nanoparticles was increased with increase in the concentration of the polymer. as shown in Table No-5 and Figure No-9.

Table No. 5: Results of drug entrapment efficiency and particle size

Sr. No.	Formulation Batches	Particle size(nm)	Drug EE (%)
01	ATL1	698.3	86.57±0.012
02	ATL2	637.5	87.91±0.028
03	ATL3	816.2	88.17±0.26
04	ATL4	735.6	89.30±0.22
05	ATL5	763.9	83.02±0.18
06	ATL6	612.9	85.56±0.015
07	ATL7	879.2	86.23±0.22
08	ATL8	923.1	88.62±0.1
09	ATL9	712.7	91.21±0.11

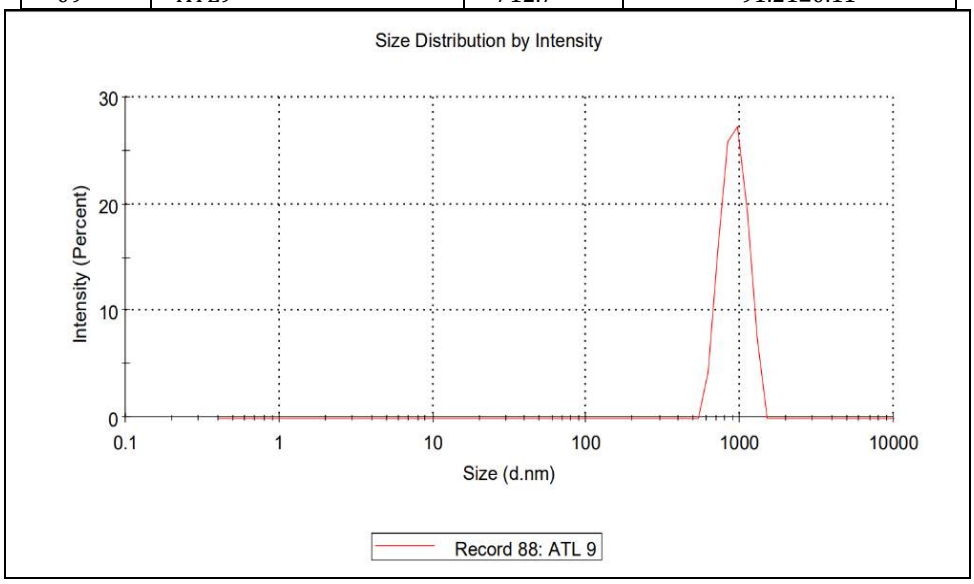

Fig No. 9: Particle size distribution of Atenolol nanoparticles of ATL9 formulation

Surface Charge:
The surface charge of Atenolol-loaded polymeric nanoparticles was analyzed using a Malvern Zeta analyzer, and the zeta potential was found to be -30.5 mV hence the formulation is stable. The zeta potential distribution results are shown in Figure 10.

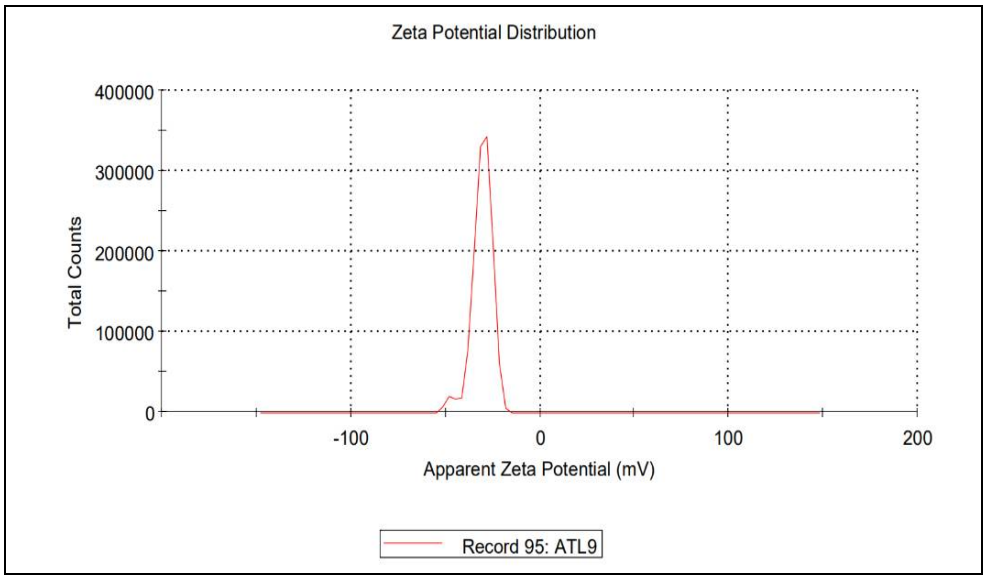

Fig No. 10: Zeta potential distribution of Atenolol nanoparticles of ATL9 formulation

Differential Scanning Calorimetry Analysis:
The DSC analysis is the most widely used calorimetric technique to characterise the physical state of drug in the formulations. Here the DSC study was carried on pure drug and ATL9 formulation and the thermograms are shown in the Figure No-11 and 12. Pure drug Atenolol exhibits a single sharp endothermic peak at 145.950C due to its glass transition temperature. The optimized formulation has shown sharp endothermic peak at 134.490C. This indicates that the drug was amorphously distributed in the formulations and there is no interaction between the drug and polymer.

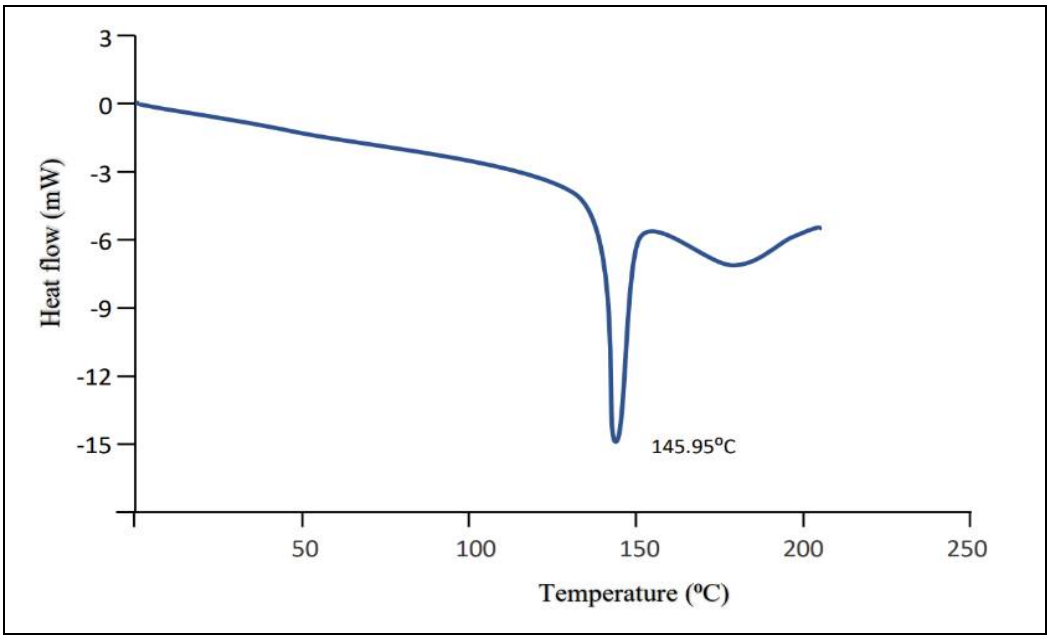

Fig No. 11: DSC spectra of Pure drug

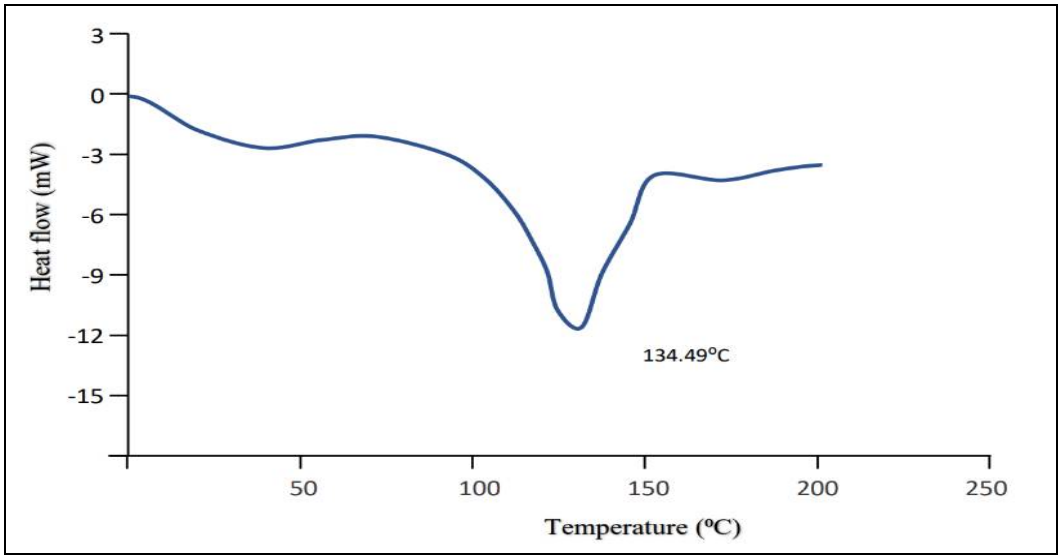

Fig No. 12: DSC spectra of ATL 9

***In-vitro* Drug release Study:**

The In-vitro drug release study was performed using type 2 dissolution test apparatus in pH 6.8 Phosphate buffer. The dissolution profile of the Atenolol Nanoparticles was given in the table No-6 to 9 and figure No- 13 to 16 the table shows the in-vitro drug release data for the formulation ATL 1 to ATL 9 was found to be 94.72%, 91.83%, 88.01%, 84.91%, 92.56%, 86.87%, 80.39%, 79.65% and 87.18% respectively at the end of 24 hour. Formulation 'ATL 9' shows the drug release of 87.18 % compare to other formulations

The release kinetics was evaluated by making use of Zero order, First order, Higuchi's model and Peppas model. Here the highest correlation coefficient R2 valve are considered, the release data of formulations seems to fit better with zero order and Higuchi model as the evident shown in table No-10. The drug release kinetics of all formulations had higher linearity in zero order compared against first order kinetic plot. This indicates the rate of release is independent of concentration and is constant over time.

The drug release of Nanoparticles Formulation follows Peppa's diffusion kinetics with control release mechanism. By fitting in the Korsemeyer- Peppa's equation the release kinetics follows non Fickian kinetics. If the 'n' values of Korsemeyer- Peppa's equation below 0.5, this indicates Fickian kinetics. If the 'n' values of Korsemeyer- Peppa's equation are in between 0.5 to 1, this indicates non Fickian kinetics. Here the Nanoparticles Formulation release kinetics are fitted in Korsemeyer- Peppa's equation. 'n' values are in between 0.55 to 0.87, so the release is following non Fickian diffusion kinetics. The 'n' values and R2 values of all nine Nanoparticles formulations are mentioned in table No-10.

When the release data were analyzed as per zero order and Peppas kinetic models, Atenolol release from the prepared Nanoparticles employing Eudragit RS100 and Eudragit RSPO obeyed Peppas model kinetics. Regression coefficient R2 values were higher in zero order model when compared to those first order model.

The short-term stability studies were carried out as per ICH guidelines on the most satisfactory formulation ATL 9 at 40±20C and 75% RH for a period of 45 days to assess short term stability as per ICH guidelines. At fixed time, the formulation was evaluated after for drug entrapment efficiency and in-vitro drug profile. Drug entrapment efficiency study shows that there is no significant changes in drug content.

In-vitro drug release profiles found to super impossible with the initial results. Therefore, the ATL 9 formulation is stable.

Table No. 6: In-vitro drug release of Atenolol from formulations ATL 1, ATL 2, ATL 3, ATL 4, ATL 5, ATL 6, ATL 7, ATL 8, and ATL 9 was conducted in phosphate buffer with a pH of 6.8.

Time (hrs.)	% Drug Release (n=9)								
	ATL 1 %DR	ATL 2 %DR	ATL 3 % DR	ATL 4 %DR	ATL 5 %DR	ATL 6 %DR	ATL 7 %DR	ATL 8 %DR	ATL 9 %DR
0	0	0	0	0	0	0	0	0	0
0.5	07.00 ±0.032	10.28 ±0.021	11.87 ±0.021	04.98 ±0.002	05.81 ±0.015	04.21 ±0.015	02.19 ±0.015	03.21 ±0.012	04.65 ±0.047
1	11.01 ±0.011	19.47 ±0.003	22.56 ±0.011	11.44 ±0.045	11.87 ±0.026	09.57 ±0.021	03.11 ±0.021	04.51 ±0.028	09.54 ±0.098
1.5	14.64 ±0.029	25.75 ±0.011	27.41 ±0.035	14.12 ±0.014	15.11 ±0.029	14.89 ±0.039	15.16 ±0.038	15.91 ±0.025	15.78 ±0.047
2	21.24 ±0.014	37.18 ±0.078	38.25 ±0.086	25.68 ±0.021	25.23 ±0.011	39.01 ±0.025	25.05 ±0.027	19.19 ±0.019	25.32 ±0.035
3	37.38 ±0.024	50.58 ±0.045	41.85 ±0.023	39.87 ±0.098	37.45 ±0.015	41.12 ±0.040	39.36 ±0.039	21.42 ±0.021	30.45 ±0.012
4	52.12 ±0.051	54.98 ±0.002	58.61 ±0.045	54.15 ±0.077	59.87 ±0.039	55.05 ±0.019	41.15 ±0.012	30.86 ±0.012	33.27 ±0.045
5	74.01 ±0.072	61.74 ±0.087	71.65 ±0.048	62.35 ±0.031	61.15 ±0.027	60.08 ±0.021	60.85 ±0.035	35.57 ±0.035	49.98 ±0.078
6	77.81 ±0.016	63.71 ±0.012	77.93 ±0.072	69.76 ±.0.16	62.02 ±0.039	62.42 ±0.029	62.95 ±0.021	36.25 ±0.017	54.07 ±0.065
7	79.47 ±0.082	69.16 ±0.012	78.32 ±0.014	72.12 ±0.032	64.62 ±0.019	65.26 ±0.025	65.52 ±0.019	39.89 ±0.028	71.15 ±0.078
8	81.82 ±0.014	72.28 ±0.095	78.56 ±0.065	74.55 ±0.025	67.35 ±0.035	71.16 ±0.024	69.25 ±0.017	42.25 ±0.025	75.89 ±0.098
9	85.27 ±0.032	76.19 ±0.020	79.93 ±0.023	75.95 ±0.023	69.14 ±0.021	73.75 ±0.026	71.21 ±0.024	49.78 ±0.034	79.66 ±0.014
10	87.67 ±0.047	81.11 ±0.081	81.06 ±0.027	76.89 ±0.078	71.17 ±0.035	75.21 ±0.028	72.31 ±0.029	59.35 ±0.025	81.54 ±0.052
11	89.32 ±0.056	83.07 ±0.009	83.45 ±0.018	77.15 ±0.023	74.78 ±0.016	76.89 ±0.019	74.20 ±0034	61.15 ±0.031	84.98 ±0.091
12	90.87 ±0.071	85.62 ±0.074	85.67 ±0.017	78.22 ±0.019	75.54 ±0.025	76.11 ±0.021	75.61 ±0.039	66.57 ±0.027	86.14 ±0.022
18	91.45 ±0.092	86.21 ±0.012	87.25 ±0.037	79.89 ±0.078	79.98 ±0.087	79.19 ±0.029	76.59 ±0.045	72.98 ±0.087	92.64 ±0.015
24	94.72 ±0.081	91.83 ±0.056	88.01 ±0.056	84.91 ±0.011	92.56 ±0.059	86.87 ±0.014	80.39 ±0.089	79.65 ±0.021	87.18 ±0.035

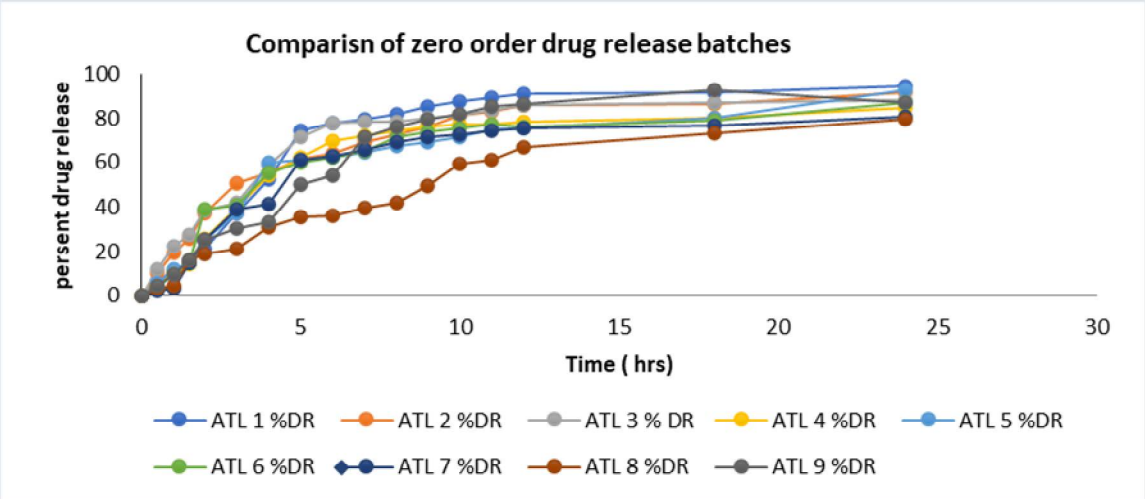

Fig No. 13: Zero order In vitro drug release profile of ATL 1, ATL 2, ATL 3, ATL 4, ATL 5, ATL 6, ATL 7, ATL 8, and ATL 9

Table No. 7: The in-vitro drug release of Atenolol from formulations ATL 1, ATL 2, ATL 3, ATL 4, ATL 5, ATL 6, ATL 7, ATL 8, and ATL 9 was analyzed for first-order kinetics in phosphate buffer at pH 6.8.

Time (hrs)	Log % Drug remaining (n=3)								
	ATL 1 Log %DR	ATL 2 Log % DR	ATL 3 Log % DR	ATL 4 Log %DR	ATL5 Log %DR	ATL6 Log %DR	ATL 7 Log %DR	ATL 8 Log %DR	ATL 9 Log %DR
0	0	0	0	0	0	0	0	0	0
0.5	1.968	1.952	1.945	1.977	1.971	1.981	1.990	1.985	1.975
1	1.949	1.905	1.888	1.947	1.945	1.956	1.986	1.979	1.956
1.5	1.92	1.878	1.849	1.924	1.92	1.909	1.913	1.914	1.912
2	1.902	1.811	1.824	1.896	1.889	1.813	1.898	1.896	1.891
3	1.805	1.704	1.772	1.827	1.832	1.763	1.83	1.866	1.849
4	1.651	1.535	1.637	1.652	1.616	1.623	1.791	1.82	1.811
5	1.445	1.427	1.437	1.472	1.578	1.59	1.604	1.795	1.718
6	1.383	1.412	1.399	1.419	1.556	1.539	1.592	1.791	1.653
7	1.354	1.403	1.336	1.396	1.536	1.515	1.55	1.741	1.489
8	1.233	1.396	1.31	1.37	1.486	1.445	1.488	1.714	1.303
9	1.138	1.291	1.303	1.363	1.475	1.419	1.428	1.627	1.286
10	1.051	1.254	1.3	1.349	1.377	1.412	1.409	1.563	1.172
11	1.033	1.181	1.268	1.343	1.339	1.399	1.394	1.551	1.005
12	0.995	1.123	1.213	1.333	1.313	1.395	1.368	1.542	0.943
18	0.938	1.085	1.138	1.317	1.252	1.339	1.331	1.397	0.798
24	0.881	1.073	1.042	1.28	1.002	1.211	1.292	1.308	1.107

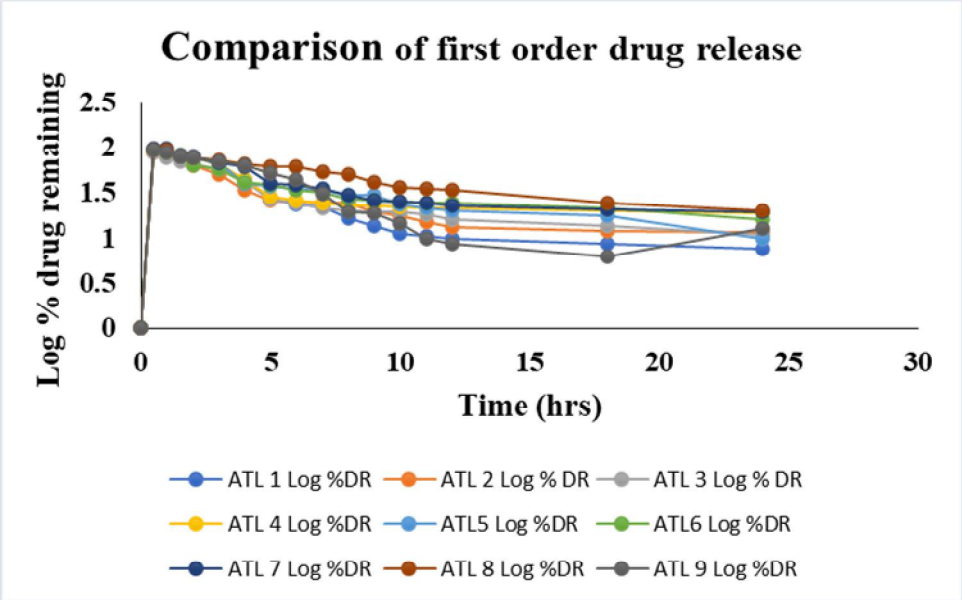

Fig No. 14: First order in-vitro drug release profile of ATL 1, ATL 2, ATL 3, ATL 4, ATL 5, ATL 6, ATL 7, ATL 8, and ATL 9

Table No. 8: Higuchi's model was used to analyze the in-vitro drug release of Atenolol from formulations ATL 1, ATL 2, ATL 3, ATL 4, ATL 5, ATL 6, ATL 7, ATL 8, and ATL 9 in phosphate buffer at pH 6.8.

√t	% Drug Release (n=9)								
	ATL1%DR	ATL2% DR	ATL3% DR	ATL4% DR	ATL5% DR	ATL6% DR	ATL7% DR	ATL8% DR	ATL9% DR
0	0	0	0	0	0	0	0	0	0
-0.301	07.00	10.28	11.87	04.98	05.81	04.21	2.19	3.21	4.65
1	11.01	19.47	22.56	11.44	11.87	09.57	3.11	4.51	9.54
1.22	14.64	25.75	27.41	14.12	15.11	14.89	15.16	15.91	15.78
1.414	21.24	37.18	38.25	25.68	25.23	39.01	25.05	19.19	25.32
1.73	37.38	50.58	41.85	39.87	37.45	41.12	39.36	21.42	30.45

2	52.12	54.98	58.61	54.15	59.87	55.05	41.15	30.86	33.27
2.23	74.01	61.74	71.65	62.35	61.15	60.08	60.85	35.57	49.98
2.44	77.81	63.71	77.93	69.76	62.02	62.42	62.95	36.25	54.07
2.64	79.47	69.16	78.32	72.12	64.62	65.26	65.52	39.89	71.15
2.82	81.82	72.28	78.56	74.55	67.35	71.16	69.25	42.25	75.89
3	85.27	76.19	79.93	75.95	69.14	73.75	71.21	49.78	79.66
3.16	87.67	81.11	81.06	76.89	71.17	75.21	72.31	59.35	81.54
3.31	89.32	83.07	83.45	77.15	74.78	76.89	74.20	61.15	84.98
3.46	90.87	85.62	85.67	78.22	75.54	76.11	75.61	66.57	86.14
4.24	91.45	86.21	87.25	79.89	79.98	79.19	76.59	72.98	92.64
4.89	94.72	91.83	88.01	84.91	92.56	86.87	80.39	79.65	87.18

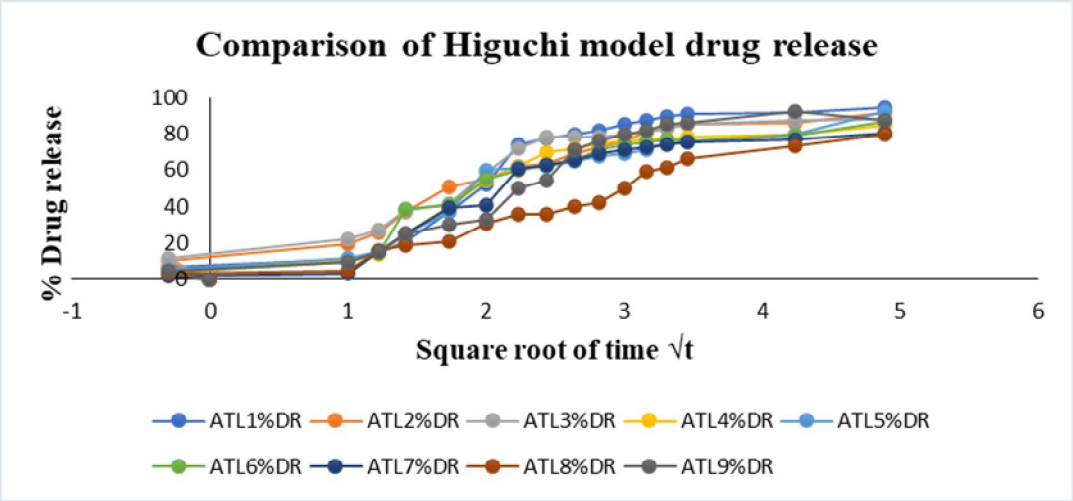

Fig No. 15: Higuchi model drug release profile of ATL 1, ATL 2, ATL 3, ATL 4, ATL 5, ATL 6, ATL 7, ATL 8, and ATL 9

Table No. 9: Peppas' model was applied to evaluate the in-vitro drug release of Atenolol from formulations ATL 1, ATL 2, ATL 3, ATL 4, ATL 5, ATL 6, ATL 7, ATL 8, and ATL 9 in phosphate buffer at pH 6.8.

Log time	Log % Drug Release (n=9)								
	ATL 1 Log % D R	ATL 2 Log % D R	ATL 3 Log % D R	ATL 4 Log % D R	ATL 5 Log % D R	ATL 6 Log % D R	ATL7 Log % D R	ATL8 Log % D R	ATL9 Log % D R
0	0	0	0	0	0	0	0	0	0
-0.301	0.845	1.011	1.074	0.697	0.764	0.624	0.340	0.506	0.667
0	1.041	1.287	1.353	1.058	1.074	0.980	0.492	0.654	0.979
0.171	1.164	1.410	1.437	1.149	1.401	1.172	1.180	1.021	1.198
0.30	1.327	1.570	1.582	1.409	1.573	1.591	1.398	1.283	1.403
0.477	1.572	1.703	1.621	1.600	1.777	1.614	1.595	1.330	1.483
0.602	1.717	1.741	1.767	1.733	1.786	1.740	1.614	1.489	1.522
0.698	1.869	1.790	1.855	1.794	1.792	1.778	1.784	1.551	1.698
0.778	1.891	1.801	1.891	1.858	1.810	1.795	1.798	1.559	1.732
0.845	1.900	1.839	1.893	1.872	1.828	1.814	1.816	1.660	1.852
0.903	1.912	1.859	1.895	1.877	1.839	1.852	1.840	1.625	1.880
0.954	1.930	2.154	1.902	1.881	1.852	1.867	1.852	1.689	1.901
1	1.942	1.909	1.908	1.887	1.873	1.876	1.859	1.773	1.911
1.04	1.950	1.919	1.921	1.891	1.878	1.885	1.870	1.786	1.929
1.079	1.958	1.932	1.932	1.902	1.902	1.881	1.878	1.823	1.935
1.255	1.961	1.935	1.940	1.918	1.941	1.898	1.884	1.863	1.966
1.380	1.976	1.962	1.872	1.924	1.966	1.938	1.905	1.901	1.940

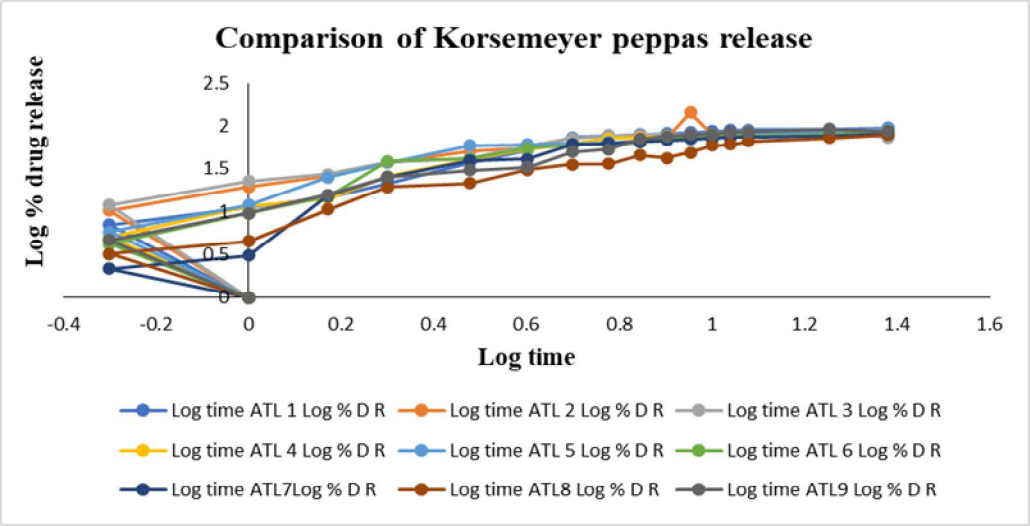

Fig No. 16: Peppas model drug release profile of ATL 1, ATL 2, ATL 3, ATL 4, ATL 5, ATL 6, ATL 7, ATL 8, and ATL 9

Table No. 10: Kinetic studies of Atenolol Nanoparticles

Formulation code	Zero order Equation		First order		Higuchi model	Peppas Equation	
	n	R^2	N	R^2	R^2	n	R^2
ATL1	4.245	0.674	0.055	0.780	0.846	0.752	0.911
ATL2	3.529	0.691	0.035	0.904	0.875	0.574	0.909
ATL3	3.286	0.764	0.033	0.899	0.922	0.553	0.965
ATL4	3.558	0.847	0.029	0.793	0.952	0.723	0.970
ATL5	3.714	0.844	0.033	0.929	0.966	0.645	0.971
ATL6	3.845	0.847	0.027	0.876	0.957	0.862	0.960
ATL7	3.443	0.941	0.028	0.923	0.979	0.797	0.982
ATL8	3.579	0.905	0.024	0.947	0.976	0.816	0.969
ATL9	3.396	0.957	0.020	0.887	0.961	0.870	0.975

Stability Study Report:

The prepared nanoparticles were stored in screw-capped HDPE bottles at 40±2°C and 75% relative humidity (RH) for 45 days. After this storage period, the product was evaluated for drug entrapment efficiency and drug release following the previously described methods. The results are presented in Table 11.

Table No. 11: Drug entrapment efficiency

Formulation Code	Drug entrapment efficiency	
	Before stability test	After stability test
ATL 9	91.21	90.92

***In-vitro* Dissolution study:**

Dissolution Study of optimized Nanoparticle was studied according to earlier procedure and determined drug release rate.

Table No. 12: *In-vitro* Dissolution study

Formulation code	Percentage of drug release	
	Before stability test	After stability test
ATL9	87.18	87.06

CONCLUSION

The results indicate that biocompatible polymers such as Eudragit RS 100 and Eudragit RSPO are effective in formulating nanoparticles with high entrapment efficiency and practical yield. Particle size analysis revealed that the nanoparticles ranged from 612.9 to 923.1 nm and exhibited favorable flow properties. Scanning electron microscopy confirmed that the nanoparticles had a smooth surface. In-vitro drug release demonstrated that the nanoparticles effectively sustained release for over 24 hours. The formulation showed stability in short-term stability studies. Pharmacokinetic analysis suggested that the

in-vitro drug release of the formulations adhered to the Peppa's model, with a non-Fickian release mechanism. Based on the in-vitro and stability study results, further in-vivo and pharmacokinetic studies are recommended. Among the formulations, ATL 9 was selected as the optimized formulation due to its excellent morphological features, drug entrapment efficiency, and drug release profile.

ACKNOWLEDGEMENT

My parents, Mr. Rajashekhara J S and Mrs. Yashoda V, along with my sister Mrs. Jyothi Kuber and brother-in-law Mr. Kuber, have provided unwavering emotional and moral support throughout my postgraduate studies. This thesis would not have been possible without their encouragement and understanding. Their support was crucial in helping me complete this work.

REFERENCES

1. Ganesh K, Archana D. (2013). Review Article on Targeted Polymeric Nanoparticles: An Overview. Am J Adv Drug Deliv [Internet].;3(3):196–215. Available from: www.ojadd.com
2. Anu Mary Ealia S, Saravanakumar MP. (2017). A review on the classification, characterisation, synthesis of nanoparticles and their application. IOP Conf Ser Mater Sci Eng [Internet]. ;263:032019. Available from: https://iopscience.iop.org/article/10.1088/1757-899X/263/3/032019
3. Messerli FH, Williams B, Ritz E. (2007). Essential hypertension. Lancet [Internet]. Aug;370(9587):591–603. Available from: https://linkinghub.elsevier.com/retrieve/pii/S0140673607612999
4. Mancia G, Grassi G, Zanchetti A. (2006). New-onset diabetes and antihypertensive drugs. J Hypertens [Internet]. Jan;24(1):3–10. Available from: https://journals.lww.com/00004872-200601000-00002
5. Chourasiya V, Bohrey S, Pandey A. (2016). Formulation, optimization, characterization and in-vitro drug release kinetics of atenolol loaded PLGA nanoparticles using 3 3 factorial design for oral delivery. Mater Discov [Internet].;5:1–13. Available from: https://linkinghub.elsevier.com/retrieve/pii/S235292451630031X
6. Castañeda L. A (2020). Facile Method for Formulation of Atenolol Nanocrystal Drug with Enhanced Bioavailability. In: Nanocrystalline Materials [Internet]. IntechOpen;. Available from: https://www. intechopen. com/ books /nanocrystalline-materials/a-facile-method-for-formulation-of-atenolol-nanocrystal-drug-with-enhanced- bioavailability
7. Zur Mühlen A, Schwarz C, Mehnert W. (1998). Solid lipid nanoparticles (SLN) for controlled drug delivery - Drug release and release mechanism. Eur J Pharm Biopharm. ;45(2):149–55.
8. Khan SA, Khan SB, Khan LU, Farooq A, Akhtar K, Asiri AM. (2018). Fourier transform infrared spectroscopy: Fundamentals and application in functional groups and nanomaterials characterization. Handb Mater Charact. ;317–44.
9. Shevalkar G, Vavia P. (2019). Solidified nanostructured lipid carrier (S-NLC) for enhancing the oral bioavailability of ezetimibe. J Drug Deliv Sci Technol [Internet]. 53(April):101211. Available from: https://doi.org/10.1016/ j.jddst.2019.101211
10. Yokoyama M, Satoh A, Sakurai Y, Okano T, Matsumura Y, Kakizoe T, et al. (1998). Incorporation of water-insoluble anticancer drug into polymeric micelles and control of their particle size. J Control Release. 13;55(2–3):219–29.
11. Wang F, Yang Z, Liu M, Tao Y, Li Z, Wu Z, et al. (2020). Facile nose-to-brain delivery of rotigotine-loaded polymer micelles thermosensitive hydrogels: In vitro characterization and in vivo behavior study. Int J Pharm. 15;577.
12. Nour SA, Abdelmalak NS, Naguib MJ, Rashed HM, Ibrahim AB. (2016). Intranasal brain-targeted clonazepam polymeric micelles for immediate control of status epilepticus: in vitro optimization, ex vivo determination of cytotoxicity, in vivo biodistribution and pharmacodynamics studies. Drug Deliv. 21;23(9):3681–95.
13. Sipos B, Szabó-Révész P, Csóka I, Pallagi E, Dobó DG, Bélteky P, et al. (2020). Quality by design based formulation study of meloxicam-loaded polymeric micelles for intranasal administration. Pharmaceutics.1;12(8):1–29.
14. Rajput AP, Butani SB. (2019). Resveratrol anchored nanostructured lipid carrier loaded in situ gel via nasal route: Formulation, optimization and in vivo characterization. J Drug Deliv Sci Technol.1;51:214–23.
15. Wavikar PR, Vavia PR. (2015). Rivastigmine-loaded in situ gelling nanostructured lipid carriers for nose to brain delivery. J Liposome Res.25(2):141–9.
16. Soliman SM, Sheta NM, Ibrahim BMM, El-Shawwa MM, Abd El-Halim SM. (2020). Novel intranasal drug delivery: Geraniol charged polymeric mixed micelles for targeting cerebral insult as a result of Ischaemia/Reperfusion. Pharmaceutics. 1;12(1).12-19
17. U. G, PATIL A, G. H. (2023). Formulation and Evaluation of Nanoparticle Drug Delivery System For Treatment of Hypertension. Int J Appl Pharm [Internet].7;90–7.
18. International Council for Harmonisation. International Conference on Harmonisation (ICH). Guidance for industry: Q1A(R2) Stability Testing of New drug Substances and Products. ICH Harmon Tripart Guidel. 2003;4(February):24.